DALTON

Interaction mode of bridging 'C_2' units in dinuclear complexes of late transition metals in low oxidation states: a theoretical approach †

Paola Belanzoni,[a] Nazzareno Re,[a] Antonio Sgamellotti *,[a] and Carlo Floriani [b]

[a] *Dipartimento di Chimica, Università di Perugia, via Elce di Sotto 8, I-06123 Perugia, Italy*
[b] *Institut de Chimie Minérale et Analytique, BCH Université de Lausanne, CH-1015, Lausanne, Switzerland*

The mode of interaction of bridging 'C_2' units in dinuclear $L_mMC_2ML_m$ complexes of late transition metals in low oxidation states, for which only an acetylenic structure has been experimentally observed, has been studied. Density functional calculations were carried out on the model complexes $[\{MCl_n(CO)_{m-n}\}_2(\mu\text{-}C_2)]$ (M = Cr, Mn, Fe or Co; $m = 4$ or 5; $n = 0$ or 1) and allowed clarification of why only the acetylenic structure is found and most of the experimentally known compounds show a d^7 configuration of the ML_m metal fragment.

Organometallic complexes in which two transition-metal atoms are bonded by μ-acetylide bridges, $L_mMC_2ML_m$, have recently received much interest.[1–3] Indeed, they constitute a first step in the synthesis of carbon forms stabilized by transition-metal complexes. The C_2 unit bridging two metals may be considered the most simple synthetic building block in this respect [3–16] and is a fragment which has been known for a long time and can easily be accessed both from acetylene and ethylene. Several $\mu\text{-}C_2$ bridged dinuclear complexes have been synthesized with structures consistent with all the three possible valence-bond descriptions [2] (see Scheme 1), although most contain an acetylenic μ-C≡C bridge.

Very few theoretical investigations have been performed on $\mu\text{-}C_2$ bridged dinuclear complexes,[4,5,8] and are mainly of semi-empirical character. In a recent paper [17] we will refer as paper I we carried out density functional theory (DFT) calculations on a wide class of $\mu\text{-}C_2$-bridged dinuclear complexes of early transition metals giving a qualitative interpretation of the bonding that occurs between the two metal atoms and the bridging C_2 ligand in terms of a simple molecular orbital scheme for four-center M–C–C–M π and δ interactions (see also refs. 18–21). Moreover, in that paper we identified two main classes of $\mu\text{-}C_2$-bridged complexes, depending on the nature of the metal, its d configuration in the ML_m fragment and the nature of the other ligands. A first class, we called class I, is constituted by early transition metals (those of the titanium, vanadium and chromium triads) in high oxidation states with mainly π-donor ligands, like RO^-, often in a pseudo-tetrahedral co-ordination.[3–7] For this class of complexes all three possible valence-bond structures have been found depending on the metal d configuration. A second class, we called class II, is constituted by mid-to-late transition metals (from the manganese triad to the right) in low oxidation states with mainly π-acceptor ligands (like carbonyl or phosphines), often in a pseudo-octahedral co-ordination.[3,8–16] For this class of complexes only the acetylenic μ-C≡C structure has been found, irrespective of the metal d configuration. It is worth noting that for most of the synthesized compounds belonging to class II the ML_m fragment has a d^7 configuration with few (essentially d^9 and d^5) exceptions. Depending on the oxidation state and the nature of the ligands, metal systems of the borderline chromium triad can be placed in both classes. Few complexes of the chromium triad in low oxidation states with π-acceptor ligands have been synthesized and they behave as members of the second class.[12,13]

† *Non-SI unit employed*: eV ≈ 1.60×10^{-19} J.

M–C≡C–M
M=C=C=M
M≡C–C≡M

Scheme 1

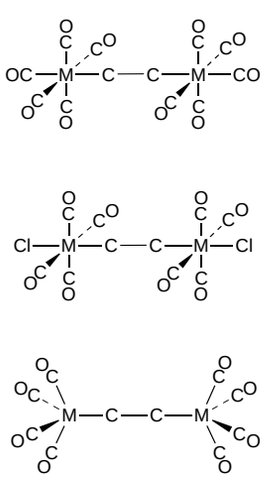

Fig. 1 Geometrical structures of the model complexes

In paper I we studied a series of model complexes belonging to class I, developing a few simple criteria which enable one to predict the structure of the relevant μ-acetylides on the basis of the metal fragment d configuration, the nature of the metal, its oxidation state, and the nature of the ligands. This paper addresses the theoretical study of class II complexes. In particular we have pointed out the reasons why only the acetylenic $\mu\text{-}C_2$ form is observed and why the d^7 fragment configuration is found so often. We have performed linear combination of atomic orbitals (LCAO) density functional calculations on a series of $[\{MCl_n(CO)_{m-n}\}_2(\mu\text{-}C_2)]$ (M = Cr, Mn, Fe or Co; $m = 4$ or 5; $n = 0$ or 1) complexes, see Fig. 1, as models of the class of μ-acetylide-bridged complexes constituted by mid-to-late transition metals in low oxidation states, with π-acceptor ligands in a pseudo-octahedral co-ordination. The shift of M from Cr to Co and of n from 0 to 1 permitted us to investigate both the effect of the change of the nature of the transition metal and of the variation of the fragment d configuration. We have found optimized structures consistent with essentially only the acetylenic $\mu\text{-}C_2$ form, giving a rationale for the special occurrence of the d^7 metal configuration.

Table 1 Metal d configurations, complex configurations and energies (with respect to atoms) for all the considered complexes

Complex	Metal d configuration	Complex configuration	State	Energy/eV
$[\{Cr(CO)_5\}_2(\mu\text{-}C_2)]$	d^6	$(9e_u)^2$	$^3A_{1g}$	−187.64
$[\{Mn(CO)_5\}_2(\mu\text{-}C_2)]$	d^7	$(9e_u)^4$	$^1A_{1g}$	−188.79
$[\{Fe(CO)_5\}_2(\mu\text{-}C_2)]$	d^8	$(9e_u)^4(5b_{1g})^2$	$^1A_{1g}$	−181.13
$[\{Fe(CO)_4\}_2(\mu\text{-}C_2)]$	d^8	$(8e_u)^2$	$^3A_{1g}$	−154.48
$[\{Co(CO)_4\}_2(\mu\text{-}C_2)]$	d^9	$(8e_u)^4$	$^1A_{1g}$	−152.15
$[\{MnCl(CO)_4\}_2(\mu\text{-}C_2)]$	d^6	$(9e_u)^2$	$^3A_{1g}$	−162.05
$[\{FeCl(CO)_4\}_2(\mu\text{-}C_2)]$	d^7	$(9e_u)^4$	$^1A_{1g}$	−160.97
$[\{CoCl(CO)_4\}_2(\mu\text{-}C_2)]$	d^8	$(9e_u)^4(5b_{1g})^2$	$^1A_{1g}$	−154.10

Table 2 Optimized geometrical parameters of $[\{M(CO)_5\}_2(\mu\text{-}C_2)]$ (M = Cr or Mn) and $[\{M(CO)_4\}_2(\mu\text{-}C_2)]$ complexes (M = Fe or Co). Bond distances in Å, angles in °

Molecule	Parameter	NLDA
$[\{Cr(CO)_5\}_2(\mu\text{-}C_2)]$	$Cr–CO_{eq}$	1.941
	$Cr–CO_{ax}$	1.953
	Cr–CC	1.916
	C–C	1.275
	$C–O_{eq}$	1.150
	$C–O_{ax}$	1.152
	$CC–Cr–CO_{eq}$	87.5
$[\{Mn(CO)_5\}_2(\mu\text{-}C_2)]$	$Mn–CO_{eq}$	1.870
	$Mn–CO_{ax}$	1.855
	Mn–CC	2.014
	C–C	1.228
	$C–O_{eq}$	1.147
	$C–O_{ax}$	1.155
	$CC–Mn–CO_{eq}$	84.8
$[\{Fe(CO)_4\}_2(\mu\text{-}C_2)]$	Fe–CO	1.838
	Fe–CC	1.902
	C–C	1.239
	C–O	1.149
	CC–Fe–CO	103.4
$[\{Co(CO)_4\}_2(\mu\text{-}C_2)]$	Co–CO	1.808
	Co–CC	1.969
	C–C	1.229
	C–O	1.150
	CC–Co–CO	104.3

Table 3 Optimized geometrical parameters of $[\{MCl(CO)_4\}_2(\mu\text{-}C_2)]$ complexes, M = Mn or Fe. Bond distances in Å, angles in °

Molecule	Parameter	NLDA
$[\{MnCl(CO)_4\}_2(\mu\text{-}C_2)]$	Mn–CO	1.895
	Mn–CC	1.845
	C–C	1.258
	Mn–Cl	2.314
	C–O	1.145
	CC–Mn–CO	88.9
$[\{FeCl(CO)_4\}_2(\mu\text{-}C_2)]$	Fe–CO	1.842
	Fe–CC	1.942
	C–C	1.229
	Fe–Cl	2.327
	C–O	1.143
	CC–Fe–CO	89.0

Computational Details

All the calculations reported in this paper are based on the ADF (Amsterdam density functional) program package described elsewhere.[22–24] The molecular orbitals were expanded in an uncontracted double-ζ slater atomic orbital (STO) basis set for all atoms with the exception of the transition-metal orbitals for which we used a double-ζ STO basis set for 3s and 3p and a triple-ζ STO basis set for 3d and 4s. As polarization functions, one 4p, one 3d and one 2p STO were used for transition metals, O and C, and H, respectively. The cores (Cr, Mn, Fe, Co: 1s–2p. C, O: 1s) were kept frozen.

The local density approximation (LDA) exchange-correlation potential and energy were used, together with the Vosko–Wilk–Nusair parametrization[25] for homogeneous electron–gas correlation, including Becke's non-local correction[26] to the local exchange expression and Perdew's non-local correction[27] to the local expression of correlation energy (NLDA). Molecular structures were optimized by the NLDA method in D_{4h} symmetry. It has been demonstrated how non-local corrections improve optimized geometries of transition-metal complexes, especially metal–ligand bond lengths, otherwise almost uniformly too short (by about 0.05 Å) if calculated by local methods.[28]

Results

The considered complexes can be grouped in two series, $[\{M(CO)_m\}_2(\mu\text{-}C_2)]$ and $[\{MCl(CO)_4\}_2(\mu\text{-}C_2)]$, where the oxidation state of the metal differs by one unit. The number of carbonyl ligands, m, has been taken so as to have a pseudo-octahedral co-ordination around the metal where allowed by the 18-electron rule as found for most experimentally characterized compounds. We took $m = 5$ for Cr–Fe (first series) and Mn–Co (second series), thus considering also 19-electron complexes. Moreover, within the first series, we have considered the compounds of Fe and Co with $m = 4$ (pseudo-square-pyramidal co-ordination). In Table 1 we report all the considered complexes together with the d″ configuration of the metal fragment and the calculated ground states with the corresponding electron configurations and energies.

We see that the ground state is a singlet, $^1A_{1g}$, or a triplet, $^3A_{1g}$, depending on the d″ configuration of the metal fragment. In particular, we have found a singlet ground state for d^7 and d^9 configurations and a triplet ground state for d^6 and d^8 configurations. For 19-electron complexes with d^8 configuration several singlet and triplet states have been found almost degenerate with the $^1A_{1g}$ ground state.

The optimized geometrical parameters of all the considered compounds are shown in Tables 2 and 3. The geometries for pseudo-octahedral complexes with a d^8 configuration have not been optimized because of frequent swapping of orbitals which occurred during the optimization causing convergence problems. This is due to the near degeneracy of many occupied and virtual orbitals which leads to swapping between excited states. Rough geometries found in non-converged optimizations are very close to those for d^7 complexes. Table 2 illustrates the optimized geometries in the $[\{M(CO)_m\}_2(\mu\text{-}C_2)]$, M = Cr, Mn, Fe or Co, series of complexes, while Table 3 illustrates those of the $[\{MCl(CO)_4\}_2(\mu\text{-}C_2)]$, M = Mn or Fe, series. The complexes $[\{Mn(CO)_5\}_2(\mu\text{-}C_2)]$ **1** and $[\{FeCl(CO)_4\}_2(\mu\text{-}C_2)]$ **2** are the most stable for the two ($n = 0$ or 1) series, respectively, and both correspond to a d^7 configuration of the metal fragment. The computed valence-energy levels, labeled according to D_{4h} symmetry, are reported in Tables 4 and 5 together with the fragment population analysis. These two molecules present the highest HOMO–LUMO (highest occupied–lowest unoccupied molecular orbital) gap in the two series and their MO diagrams will

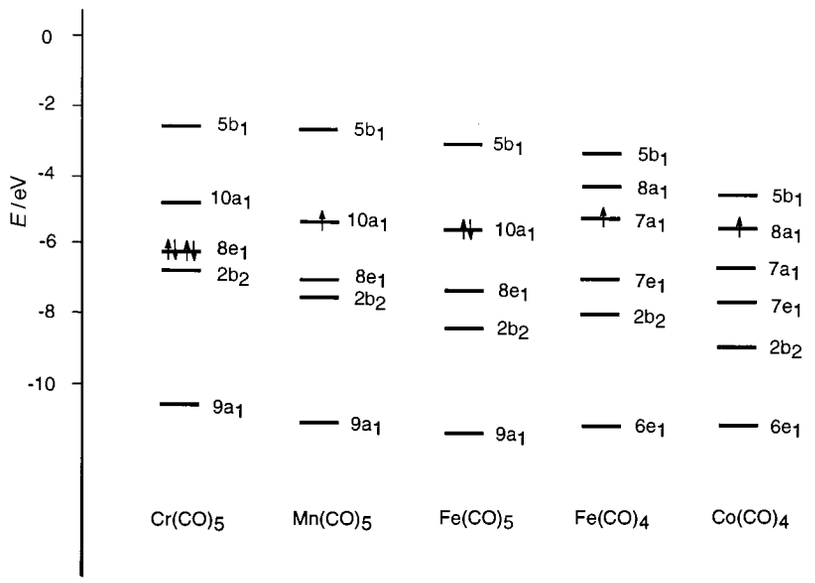

Fig. 2 Energies of the main frontier orbitals for the $M(CO)_m$ metal fragments

Table 4 Energies and composition of the $[\{Mn(CO)_5\}_2(\mu\text{-}C_2)]$ orbitals. The nature of the metal contributions is mentioned in parentheses

Orbital	*E*/eV	% Mn	% CO	% CC
$5b_{2u}$	−2.401	31 ($3d_{x^2-y^2}$)	66	
$5b_{1g}$	−2.438	25 ($3d_{x^2-y^2}$)	70	
$3b_{1u}$	−2.559	30 ($3d_{xy}$)	69	
$3b_{2g}$	−2.577	29 ($3d_{xy}$)	69	
$12a_{1g}$	−2.647		80	
$10e_u$	−2.773		91	
$11a_{2u}$	−2.774		82	
$9e_g$ LUMO	−2.810		86	
$9e_u$ (3π) HOMO	−5.853	24 ($3d_{xz,yz}$)		67 ($1\pi_u$)
$8e_g$ (2π)	−7.373	68 ($3d_{xz,yz}$)	24	
$2b_{1u}$ (2δ)	−7.679	66 ($3d_{xy}$)	31	
$2b_{2g}$ (1δ)	−7.680	66 ($3d_{xy}$)	31	
$8e_u$ (1π)	−7.742	47 ($3d_{xz,yz}$)	12	25 ($1\pi_u$)
$11a_{1g}$ [σ(M–C)]	−8.507	32 ($4p_z$, $3d_{z^2}$)	10	37 ($3\sigma_g$)
$10a_{2u}$ [σ(M–C)]	−10.046	21 ($4p_z$, $3d_{z^2}$)	17	51 ($2\sigma_u$)
$7e_g$	−11.093		77	

Table 5 Energies and composition of the $[\{FeCl(CO)_4\}_2(\mu\text{-}C_2)]$ orbitals. The nature of the metal contributions is mentioned in parentheses

Orbital	*E*/eV	% Fe	% CO	% Cl	% CC
$3b_{1u}$	−3.520	23 ($3d_{xy}$)	76		
$3b_{2g}$	−3.534	23 ($3d_{xy}$)	76		
$5b_{2u}$	−3.666	51 ($3d_{x^2-y^2}$)	37		
$5b_{1g}$	−3.679	51 ($3d_{x^2-y^2}$)	38		
$11a_{1g}$	−4.044	22 ($3d_{z^2}$)	46	21	
$10a_{2u}$ LUMO	−4.145	35 ($3d_{z^2}$)	26	24	
$9e_u$ (3π) HOMO	−6.221	35 ($3d_{xz}$)		14	50 ($1\pi_u$)
$8e_g$	−6.784	20 ($3d_{xz,yz}$)		77	
$8e_u$	−7.024	10 ($3d_{xz,yz}$)		71	15 ($1\pi_u$)
$10a_{1g}$	−8.457	16 ($4p_z$)		57	13 ($3\sigma_g$)
$7e_g$ (2π)	−8.510	62 ($3d_{xz,yz}$)	11	19	
$9a_{2u}$	−8.790	11 ($4p_z$)		68	
$7e_u$ (1π)	−8.809	52 ($3d_{xz,yz}$)	12	12	19 ($1\pi_u$)
$2b_{1u}$ (2δ)	−8.851	72 ($3d_{xy}$)	20		
$2b_{2g}$ (1δ)	−8.852	72 ($3d_{xy}$)	20		
$9a_{1g}$ [σ(M–C)]	−9.973	45 ($3d_{z^2}$)		14	27 ($3\sigma_g$)
$8a_{2u}$ [σ(M–C)]	−11.273	31 ($3d_{z^2}$)	10		42 ($2\sigma_u$)
$6e_g$	−11.842		84		

serve as a basis for the discussion of all the other complexes. Of particular relevance is also $[\{Co(CO)_4\}_2(\mu\text{-}C_2)]$ **3**, which is the most representative of the pseudo-square-co-ordinated complexes.

The electronic interaction between the C_2 unit and the metal

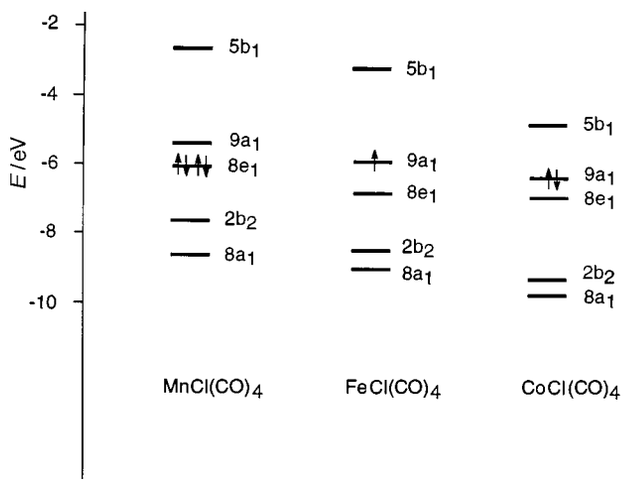

Fig. 3 Energies of the main frontier orbitals for the $MCl(CO)_4$ metal fragments

fragments has been discussed by a fragment approach in which the two metal fragments interact with a C_2 species along a common MCCM axis. Note that such an approach leads to an electron count for the metal in the $MCl_n(CO)_{m-n}$ fragments slightly different from that which would be considered in the whole dinuclear complex on the basis of formal oxidation-state assignments.

The $M(CO)_m$ and $MCl(CO)_4$ fragments have been considered in a pseudo-square-pyramidal structure, of C_{4v} symmetry, with the same geometries obtained by the optimization of the corresponding dinuclear complexes, and some of their valence MOs are reported in Figs. 2 and 3. For the $M(CO)_5$ fragments the frontier d orbitals are constituted by a lower set of three t_{2g}-like orbitals, labeled as $2b_2$ (d_{xy}) and $8e_1$ (d_{xz}, d_{yz}) in the C_{4v} point group, slightly mixed with the π* orbitals of the CO ligands, and by two higher e_g-like orbitals, labeled as $10a_1$ (d_{z^2}, p_z hybrid) and $5b_1$ ($d_{x^2-y^2}$). The $5b_1$ is of d_δ symmetry and lies at high energies due to the interactions with the equatorial CO 5σ. The other d_δ orbital, $2b_2$, is instead stabilized by the back bonding to the equatorial CO π*. The d_π orbitals, $8e_1$, remain degenerate and are stabilized by the back bonding to the axial and two of the equatorial CO π*. An analogous situation is found for the $M(CO)_4$ fragments, the main difference consisting in the lower energy of the b_1 ($d_{x^2-y^2}$) orbital due to a reduced interaction with the carbonyl ligands. Note that, at variance with the

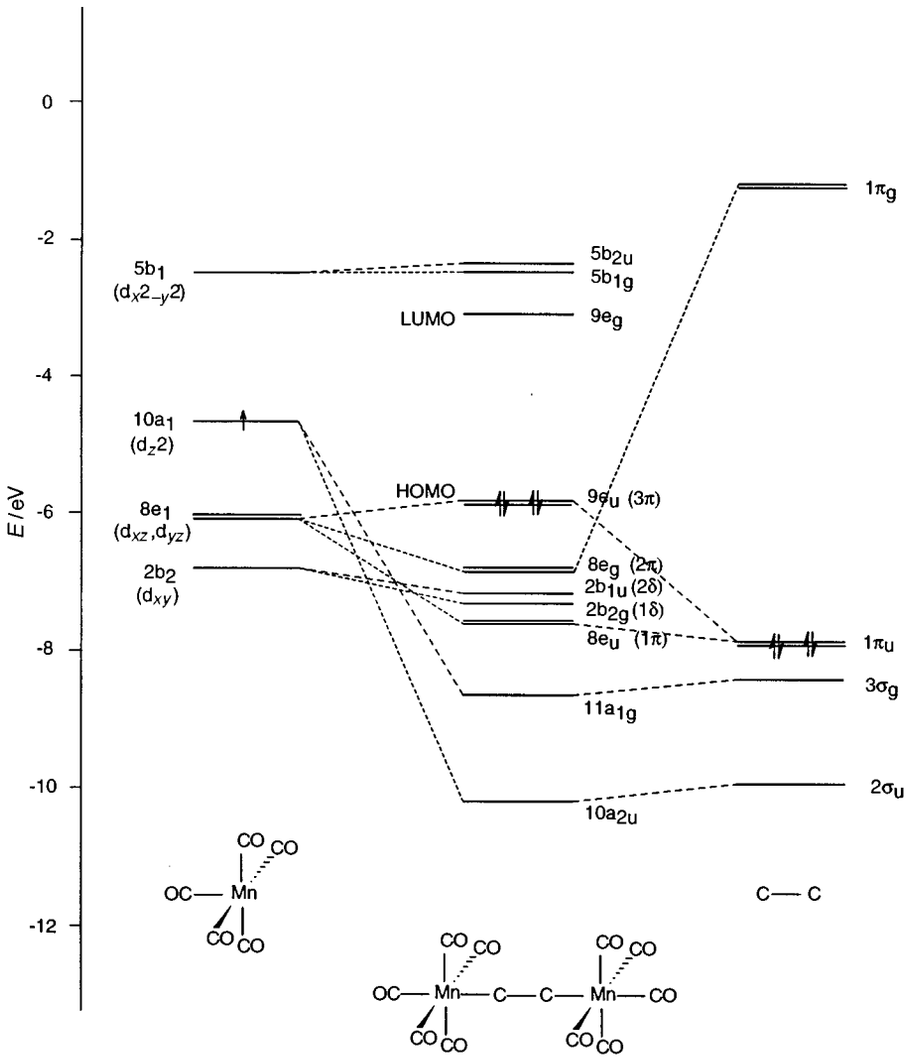

Fig. 4 Molecular orbital diagram for the $[\{Mn(CO)_5\}_2(\mu\text{-}C_2)]$ complex depicting the interactions between the frontier orbitals of $Mn(CO)_5$ and C_2

$M(CO)_5$ fragments, both the d_δ orbitals are relatively low lying. For the $MCl(CO)_4$ fragments the relative energies and the character of the frontier d orbitals are similar to those of $M(CO)_5$. They are now labeled as $2b_2$ (d_{xy}), $8e_1$ (d_{xz}, d_{yz}), $9a_1$ (d_{z^2}, p_z) and $5b_1$ ($d_{x^2-y^2}$). Owing to the higher oxidation state of the metals, M^I instead of M^0, they are all slightly shifted to lower energies.

The C_2 molecule has been considered in the $^3\Sigma_u$ state, $(1\pi_u)^4(2\sigma_u)^1(3\sigma_g)^1$ configuration, corresponding to the valence state, and its main valence orbitals are depicted on the right in Figs. 4 and 5. The singly occupied $3\sigma_g$ and $2\sigma_u$ correspond to the in- and out-of-phase combinations of the carbon sp hybrids and are of the right symmetry to interact with the metal d_σ orbitals. The HOMO $1\pi_u$ corresponds to the two orthogonal π orbitals while the LUMO $1\pi_g$ corresponds to the two π* orbitals.

We will distinguish two cases corresponding to (*i*) pseudo-octahedral and (*ii*) pseudo-square-pyramidal co-ordinations around the metal atom.

Pseudo-octahedral co-ordination

Figs. 4 and 5 show the orbital interaction diagrams for complexes **1** and **2** which are representative of the behaviour for this co-ordination. For all the considered complexes the orbitals with bonding character between metal atoms and the C_2 molecule or of metal d character can be divided into four groups.

(*i*) Two low-lying orbitals describing the σ M–C bonds, formed by the in- and out-of-phase d_σ orbitals of the $MCl_n(CO)_{5-n}$ fragments interacting with the $3\sigma_g$ and $2\sigma_u$ orbitals of C_2. Together with a lower orbital describing the C–C bond (mainly a pure $2\sigma_g$ orbital of C_2) they constitute the M–C–C–M σ skeleton.

(*ii*) A group of four metal d orbitals (two of d_δ and two of d_π character), the latter two slightly mixed with the bridging C_2 π and π* orbitals.

(*iii*) The doubly degenerate HOMO which essentially describes the two π bonds of C_2 and is mainly formed by the $1\pi_u$ orbitals of C_2 slightly interacting with the out-of-phase combination of the d_π orbitals of the metal fragments. This orbital becomes the LUMO or the singly occupied molecular orbital (SOMO) for the other complexes of the series, but remains high lying and keeps a high $\pi(C_2)$ character.

(*iv*) A group of low-lying virtual orbitals (eventually occupied for other complexes in the series) which are essentially of d_δ–π*(CO) character.

The orbitals of the latter three groups describe the metal–carbon π bonds and the metal d_δ electrons and are by far the most important: they constitute the π–δ system and will be discussed in more detail in the next section. In particular, in complex **1** the $8e_u$ and $8e_g$ essentially describe the d_π [slightly mixed with $\pi(C_2)$ and $\pi^*(C_2)$, respectively], the $2b_{2g}$, $2b_{1u}$, $5b_{1g}$ and $5b_{2u}$ the metal d_δ orbitals and the HOMO $9e_u$ essentially describes the two π bonds of C_2, slightly mixed with metal d_π orbitals. A similar situation is found for **2**, although the composition of the π–δ orbitals is significantly different (compare Tables 4 and 5)

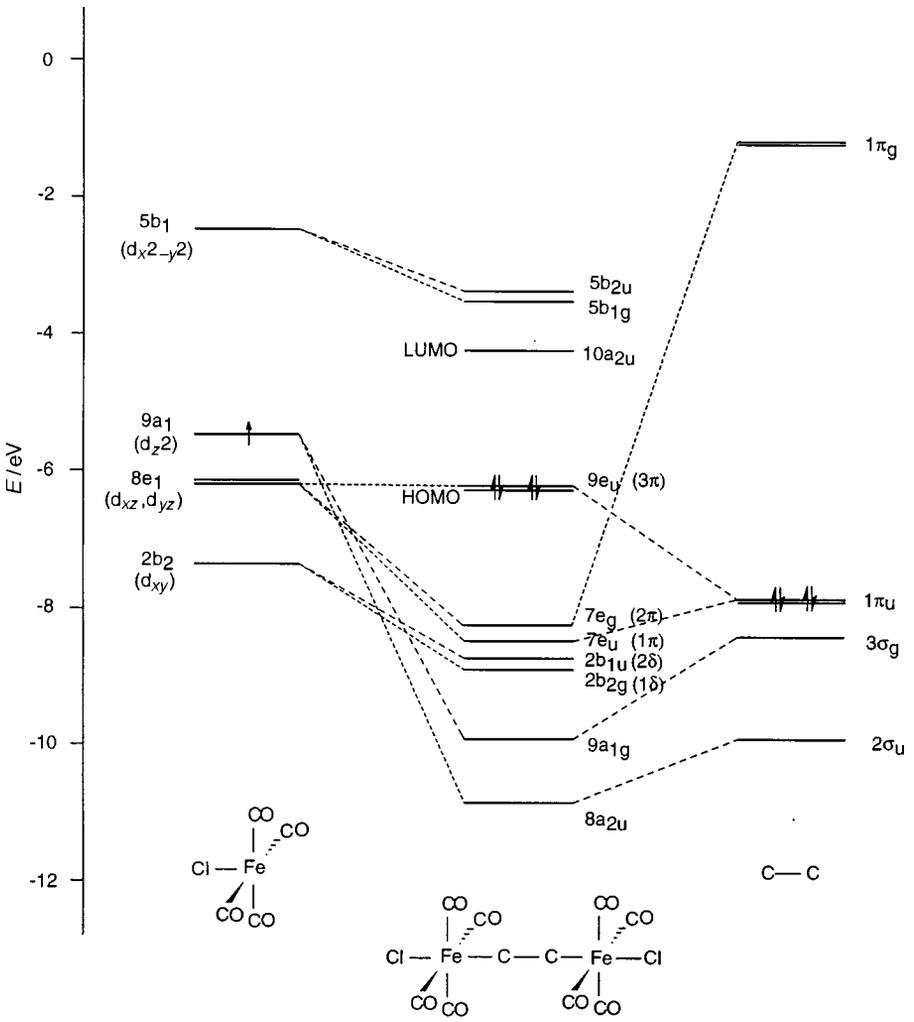

Fig. 5 Molecular orbital diagram for the $[\{FeCl(CO)_4\}_2(\mu\text{-}C_2)]$ complex depicting the interactions between the frontier orbitals of $FeCl(CO)_4$ and C_2

and the level numbering is slightly changed by the presence of M–Cl σ and π bonding and antibonding orbitals.

For complexes **1** and **2** with a d^7 configuration of the $Mn(CO)_5$ or $FeCl(CO)_4$ fragments, the HOMO is the fully occupied doubly degenerate $9e_u$ of mainly $\pi(C_2)$ character, while the LUMO is a $9e_g$ or a $10a_{2u}$ of $\pi^*(CO)$ or $\sigma^*(M–Cl)$ character, respectively. In both cases these LUMOs are almost degenerate with several other orbitals of $\pi^*(CO)$ or $\pi^*(M–Cl)$ character and a group of d_δ orbitals, strongly mixed with $\pi^*(CO)$. The ground-state configurations of all the other considered complexes ($m = 5$) can be deduced by the orbital level order in Tables 4 and 5 and are reported in Table 1. Table 1 shows that the $9e_u$ or $8e_u$ orbital is doubly occupied for $[\{Cr(CO)_5\}_2(\mu\text{-}C_2)]$ or $[\{MnCl(CO)_4\}_2(\mu\text{-}C_2)]$ with a fragment d^6 configuration while in complexes with d^8 fragment configuration the extra electrons occupy the $5b_{1g}$ orbitals of d_δ character.

Pseudo-square-pyramidal co-ordination

Fig. 6 shows the orbital interaction diagram of complex **3**, which is the most representative of the pseudo-square-pyramidal co-ordination. It is very close to those of **1** and **2**, differing primarily in the presence of two more low-lying metal orbitals of d_δ character. This difference means that the most stable closed-shell square-pyramidal complex has a d^9 fragment configuration instead of a d^7 configuration as found for pseudo-octahedral complexes. Therefore in **3** the HOMO is the fully occupied $8e_u$ orbital of mainly $1\pi_u$ character which is only doubly occupied in the $[\{Fe(CO)_4\}_2(\mu\text{-}C_2)]$ species with a d^8 fragment configuration.

Discussion

A qualitative molecular orbital interpretation

All the results presented in the previous section can be interpreted with a molecular orbital scheme for four-center M–C–C–M π and δ systems used to interpret the results of DFT calculations on class I complexes in paper I.

This is a simple molecular orbital scheme for such interactions, analogous to that proposed to explain bonding in dinitrogen-bridged transition-metal dimers[18] and to interpret the results of *ab initio* calculations on these complexes.[19–21] In such a model we assume that the metal d_{z^2} orbitals strongly interact with the sp hybrid of each carbon forming two low-lying MOs describing M–C σ bonds, while two other carbon sp hybrids form the C–C σ-bond MO at an even lower energy. The frontier orbitals involved in the bonding of the dicarbide bridge are therefore those originating from the interactions of the carbon π with the metal d_π orbitals and from the d_δ orbitals (see Scheme 2).

As long as the σ M–C–C–M skeleton is regarded as mainly constant, the variation in the M–C and C–C bond character can be attributed to changes in the nature and in the occupancy of the frontier orbitals.

For complexes of class I the unoccupied or singly occupied metal d orbitals, destabilized by their interactions with the π-donor ligands, are higher in energy than the C_2 π orbitals and the 1π level corresponds essentially to the $1\pi_u$ MO of the C_2 molecule, of C–C π bonding character.[17] Moreover, the 2π–3π orbitals possess higher metal character and the pure metal δ orbitals lie between them.

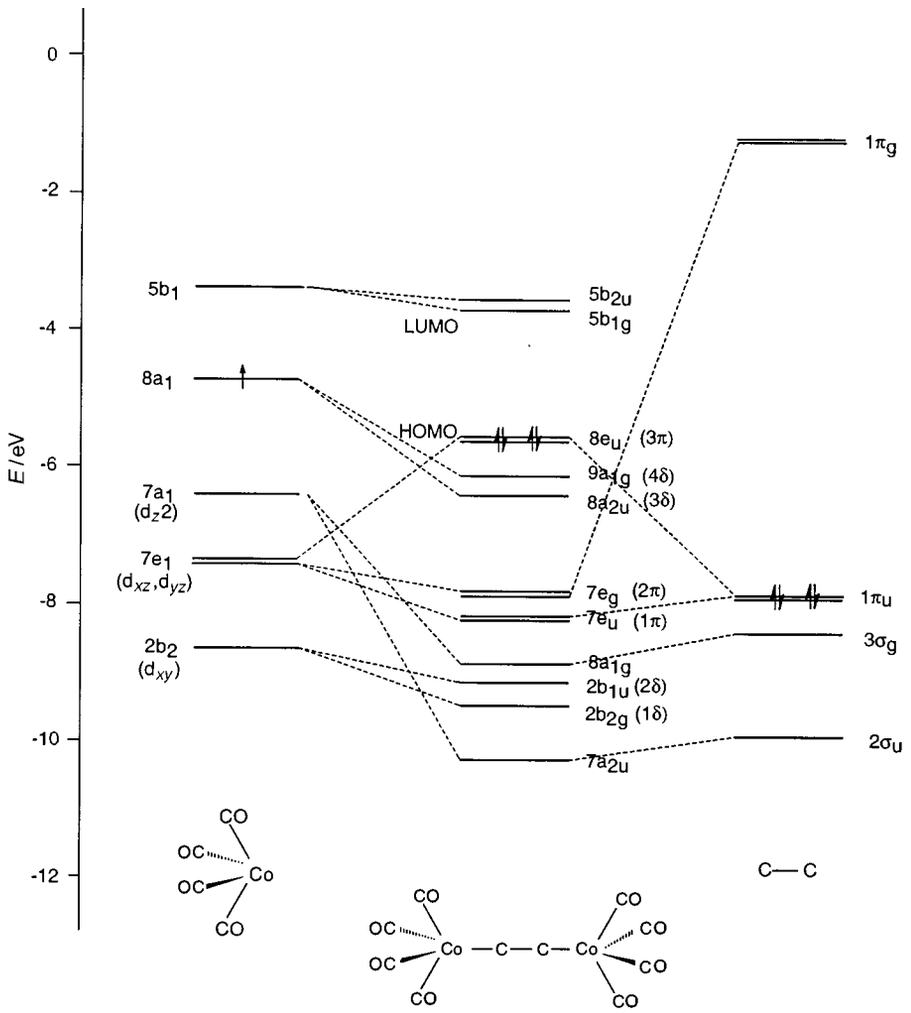

Fig. 6 Molecular orbital diagram for the [{Co(CO)$_4$}$_2$(μ-C$_2$)] complex depicting the interactions between the frontier orbitals of Co(CO)$_4$ and C$_2$

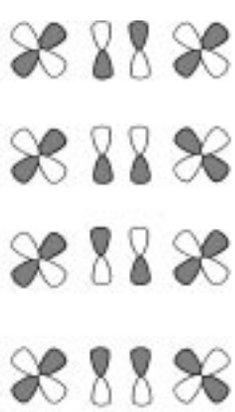

Scheme 2

The filling of these orbitals with the d electrons of the metal fragments and with the π electrons of the C$_2$ unit allows us to forecast the valence structures for the C$_2$-bridged complexes, on the basis of the metal d configuration of the ML$_m$ fragments, as summarized below.

Fragment d configuration	Bond character
d^1	M–C≡C–M
d^2	M=C=C=M
d^3	M≡C–C≡M

Such a molecular orbital model must be slightly modified to take into account the different nature of the metal fragments between the two classes. Indeed, for complexes belonging to class II, the doubly occupied metal d_π and d_δ orbitals, stabilized by interactions with π-acceptor ligands, are low in energy and close to the C$_2$ π orbitals. In this case the 1π and 2π orbitals are mainly of metal character and correspond to the symmetric and antisymmetric combinations of d_{xz} and d_{yz} orbitals only very slightly mixed with, respectively, π and π* orbitals of C$_2$. The 3π level is higher in energy and has a high π(C$_2$) contribution. Moreover, for a pseudo-octahedral eclipsed co-ordination of the metal fragment often found in this class, the $d_{x^2-y^2}$ levels are destabilized by σ interactions with equatorial CO ligands, leaving only two δ_{xy} levels at energies close to those of the 1π–3π orbitals (see Fig. 7).

The electron count for the occupancy of these levels is performed by considering a neutral C$_2$ molecule bracketed by the two metal ML$_m$ fragments. If each ML$_m$ fragment has a d^n configuration, a total of $2(n - 1) + 4$ electrons is left to occupy these π and δ frontier orbitals, four from the C$_2$ unit and $n - 1$ from each metal fragment.

We would then expect a complete filling of the $1\delta_{xy}$–$2\delta_{xy}$ and the 3π orbitals, with a singlet ground state and a formal acetylenic structure, for a d^7 configuration of the metal fragment L$_m$M. For complexes with a higher electron count the extra electrons occupy the low-lying virtual orbitals of $\delta_{x^2-y^2}$–π*(CO) character and the structure remains acetylenic. On the other hand, in complexes with a lower electron count, the electrons depopulate the 3π orbital of π(C$_2$) character and a trend towards a cumulenic M=C=C=M geometry is expected. However, these latter complexes are constituted by mid to early transition metals and cannot be strictly classified as class II. For complexes with a co-ordination number lower than six, the $d_{x^2-y^2}$ levels are less destabilized due to the reduced interaction with the ancillary ligands and four δ orbitals (two δ_{xy} and two

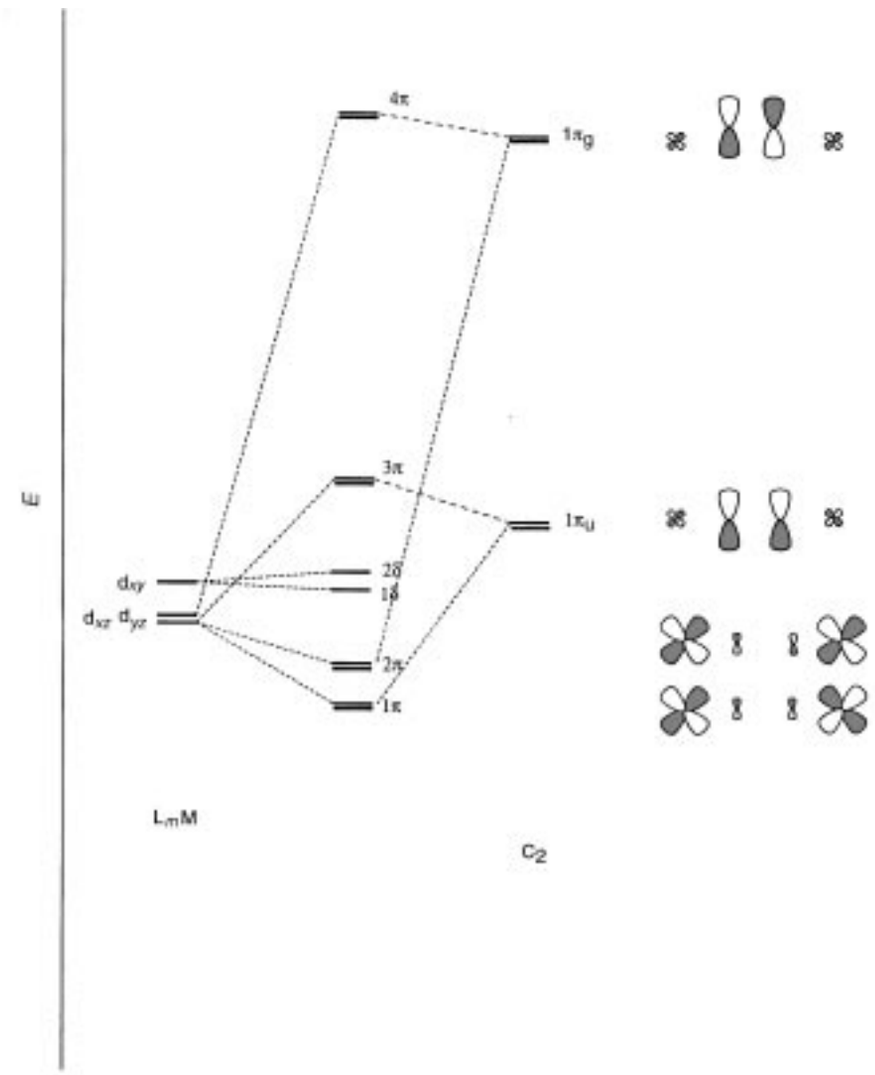

Fig. 7 Schematic molecular orbital diagram for $L_mMC_2ML_m$ complexes of class II depicting the main interactions between the frontier orbitals of L_mM and C_2

$\delta_{x^2-y^2}$) are left at energies close to those of the 1π–3π levels. In this case a stable closed-shell ground state is found for a d^9 configuration of the metal fragment. For complexes with a coordination number higher than six, both the $d_{x^2-y^2}$ and d_{xy} level are destabilized due to the interaction with more ancillary ligands and could be at energies far higher than the 3π levels leading to a stable closed-shell ground state for a d^5 configuration of the metal fragment.

Electronic structure

This qualitative Hückel-like model is supported by the results of our accurate DFT calculations. The frontier orbitals of M–C and C–C character calculated for complexes **1** and **2** correspond to the 1π–3π and 1δ–4δ orbitals the progressive occupation of which by the d electrons of the fragments determines the valence description of the M–C and C–C bonds (see Tables 4 and 5). For complex **1** (M = Mn) we have already seen the correspondence between the $8e_u$, $2b_{2g}$, $2b_{1u}$, $8e_g$, $9e_u$, $5b_{1g}$ and $5b_{2u}$ calculated levels (see Table 4) and the 1π, 1δ, 2δ, 2π, 3π, 3δ and 4δ orbitals, respectively, of the Hückel-like model. Fig. 4 may serve to show the progressive filling of the frontier orbitals in the $[\{M(CO)_5\}_2(\mu\text{-}C_2)]$ (M = Cr, Mn or Fe) series and illustrates the effect of the electron count on orbital occupation. The double degenerate $9e_u$ orbital, with an essentially $\pi(C_2)$ character, is fully occupied and is the HOMO. As the $8e_u$ (1π), $2b_{2g}$ (1δ), $2b_{1u}$ (2δ) and $8e_g$ (2π) orbitals all have an almost pure metal character, this complex has therefore a formal acetylenic M–C≡C–M structure. The next orbital to be occupied in the iron complexes, made up of d^8 fragments, is the $5b_{1g}$ or $5b_{2u}$ (3δ–4δ), with a relevant π*(CO) character, so that the acetylenic structure is maintained. When we pass to the chromium complex, with a d^6 fragment, two electrons are removed from the $9e_u$ orbital of mainly $\pi(C_2)$ character, so that a shift to a cumulenic structure is expected and actually found in the geometry optimization (see Table 2). An analogous situation, although with a slightly different orbital numbering, is found when we consider the $[\{MCl(CO)_4\}_2(\mu\text{-}C_2)]$ (M = Cr, Mn, Fe or Co) series. For complex **2** (M = Fe), the HOMO is the $9e_u$, still with main $\pi(C_2)$ character, and leads to a formal acetylenic structure. Fig. 5 shows that the progressive filling of the frontier orbitals in this series is exactly the same as discussed in the previous one, provided there is a shift of one metal to the right of the transition series. So, a formal acetylenic M–C≡C–M structure is observed for the complexes of Fe to Co, with d^7 to d^8 fragment configurations, while a trend to a cumulenic structure is expected for the complexes of Mn and Cr with d^6 and d^5 configurations in agreement with the optimized geometries (see Table 3). Fig. 6 illustrates the electronic structure of **3** and the progressive orbital occupations in the $[\{M(CO)_4\}_2(\mu\text{-}C_2)]$ complexes. Owing to the presence of four low-lying δ orbitals, the most stable closed-shell singlet is found for the cobalt complex **3**, with a d^9 electron count. The HOMO is the fully occupied $8e_u$ of mainly $1\pi_u$ (C_2) character which leads to an acetylenic structure (see Table 2). A shift to a cumulenic structure is observed for the iron complex (d^8 fragment) with the $8e_u$ only doubly occupied.

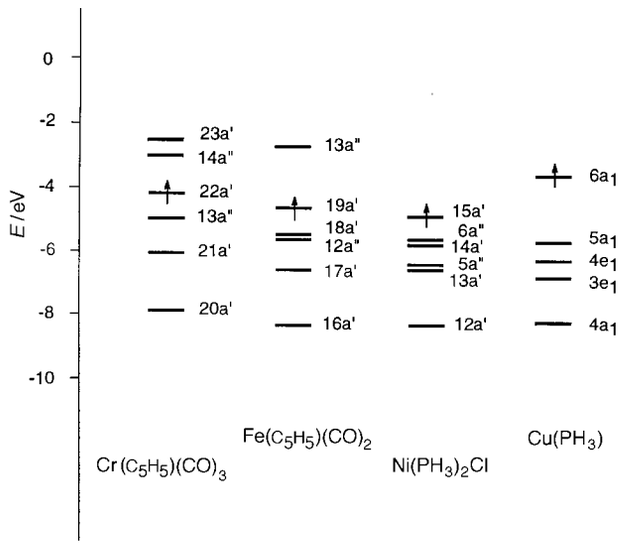

Fig. 8 Energies of the main frontier orbitals for the $Cr(C_5H_5)(CO)_3$, $Fe(C_5H_5)(CO)_2$, $Ni(PH_3)_2Cl$ and $Cu(PH_3)$ fragments

All the synthesized μ-C_2 bridged dinuclear complexes belonging to class II show an acetylenic structure, and for most of them the metal fragments have a d^7 configuration.[2] In particular, all the complexes in which the metal has in the fragment an oxidation state 0 or +1 with a pseudo-octahedral geometry and a co-ordination number five are made up by $M(CO)_5$ or $M(C_5H_5)(CO)_2$ fragments with a d^7 configuration. Complexes with a higher electron count have been observed only for co-ordinatively less saturated fragments like $M(PR_3)_2X$ (X = Cl or I; M = Pd or Pt),[14] co-ordination number three, with a d^9 configuration or $M(PR_3)$ (M = Au),[15] co-ordination number one, with a $d^{10}s^1$ configuration. Complexes with a lower electron count have been observed only for more highly co-ordinated fragments like $M(C_5H_5)(CO)_3$ (M = Cr or W),[12,13] co-ordination number six, with a d^5 configuration and show an acetylenic structure. All these behaviours can be still rationalized within the Hückel-like model if we take into account the effect of changing the co-ordination number. Indeed, as mentioned above, in the co-ordinatively less saturated complexes (co-ordination numbers three or four) one or two more d orbitals (d_δ and d_σ) per metal are lowered by the reduced interactions with ligands and the 3π fully occupied for a d^9 or d^{10} s^1 fragment configuration. On the other hand, in the co-ordinatively more saturated compounds (co-ordination number six) there is an energy lift of a d_δ orbital (due to the increased interactions with the ligands) leaving the 3π fully occupied for a d^5 fragment configuration.

A few further calculations have been performed better to investigate the electronic structure of some of the latter compounds not strictly belonging to the considered $[\{MCl(CO)_4\}_2(\mu\text{-}C_2)]$ or $[\{M(CO)_5\}_2(\mu\text{-}C_2)]$ series of complexes. First of all, DFT calculations have been carried out on the $[\{Fe(C_5H_5)(CO)_2\}_2(\mu\text{-}C_2)]$ complex, corresponding to an experimentally synthesized compound,[16] to study the change of the electronic structure due to the shift from an $FeCl(CO)_4$ to an $Fe(C_5H_5)(CO)_2$ fragment, both pseudo-octahedral and with a d^7 configuration. We found a set of frontier MOs with energies and compositions very similar to those obtained for the corresponding $[\{FeCl(CO)_4\}_2(\mu\text{-}C_2)]$ and reported in Table 4. In particular a high HOMO–LUMO gap (*ca.* 2 eV) has been found, which confirms the stability of this species. The main difference is the splitting of the degeneracy of the MOs with d_π or $\pi(C_2)$ character due to the lower symmetry of the C_{2h} group. Secondly, DFT calculations have been performed on the $Fe(C_5H_5)(CO)_2$, $Ni(PH_3)_2Cl$, $Cu(PH_3)$ and $Cr(C_5H_5)(CO)_3$ fragments to study the effect of the different geometries and co-ordination numbers on the energies of the fragment d orbitals. The energy-level diagrams for these fragments are reported in Fig. 8. In agreement with the previous qualitative forecast, the obtained results show that: (*i*) $Fe(C_5H_5)(CO)_2$ has d-energy levels very similar to those calculated for $FeCl(CO)_4$; in particular one of the two d_δ orbitals (17a′) lies at low energies and is occupied while the other one (13a″) lies at high energy and is empty; (*ii*) in $Ni(PH_3)_2Cl$ the d_δ orbitals (13a′ and 5a″) lie both at low energy and are occupied; (*iii*) in $Cu(PH_3)$ also the d_σ orbital ($5a_1$) is at low energy and occupied so that the M–C σ bond in the corresponding μ-C_2 complex will be formed by the singly occupied $6a_1$ orbital of s(Cu) character; (*iv*) in $Cr(C_5H_5)(CO)_3$ the d_δ orbitals (14a″ and 23a′) both lie at high energy and are empty.

Geometries

The calculated C–C and M–C bond distances in the $[\{M(CO)_m\}_2(\mu\text{-}C_2)]$ (M = Cr, Mn, Fe or Co) and $[\{MCl(CO)_4\}_2(\mu\text{-}C_2)]$ (M = Mn or Fe) series in Tables 2 and 3 match very well with the formal structures forecast on the basis of the Hückel-like model described above and the analysis of the electronic structure discussed in the previous paragraph. Table 2 illustrates that for the complexes of Mn and Fe of the $[\{M(CO)_m\}_2(\mu\text{-}C_2)]$ series, with d^7 and d^8 configurations of the $M(CO)_m$ fragment, the calculated C–C and M–C bond lengths are similar and correspond to an acetylenic M–C≡C–M structure. In particular, we see that the C–C bond lengths fall in the range 1.22–1.23 Å, while M–C bond lengths fall in the range 1.95–2.05 Å, close to the values reported for triple C–C and corresponding M–C single bonds, respectively. On the other hand, when we pass to the chromium species, for which the $M(CO)_5$ fragment has a d^6 configuration, there is a relevant lengthening of the C–C bond and a shortening of the M–C bond. The calculated C–C and M–C bond lengths are 1.275 and 1.916 Å which suggest a structure close to a cumulenic form. We recall that the right comparison of C–C bond lengths should be made with single, double and triple bonds between sp-hybridized carbons, *i.e.* ethyne (1.212 Å), cumulene (1.284 Å) and buta-1,3-diyne (1.384 Å), respectively. Moreover, the range of distances expected for a Cr–C double bond is 1.80–1.95 Å.

The trend of the optimized geometrical parameters calculated for the $[\{MCl(CO)_4\}_2(\mu\text{-}C_2)]$ (M = Mn or Fe) series (see Table 3) is very similar, accounting for the shift of one metal to the right of the transition series. The only relevant difference in the geometries between the two series consists in M–C bond lengths slightly shorter than those calculated for the corresponding complexes of the previous series, which can be ascribed to the higher metal oxidation state of the $MCl(CO)_4$ fragments with respect to the $M(CO)_5$ ones.

Table 2 also illustrates the optimized geometries calculated for the $[\{M(CO)_4\}_2(\mu\text{-}C_2)]$ (M = Fe or Co) complexes showing an acetylenic structure for M = Co [R(C–C) = 1.229 and R(Co–C) = 1.969 Å] and a slight shift to a cumulenic structure for M = Fe [R(C–C) = 1.239 and R(Fe–C) = 1.902 Å].

One of the theoretically considered complexes, $[\{Mn(CO)_5\}_2(\mu\text{-}C_2)]$, has been synthesized and structurally characterized.[9] The calculated parameters, R(C–C) = 1.23 and R(Mn–C) = 2.01 Å, are very close to the experimental values, 1.20 and 2.01 Å, respectively. Moreover, a slight distortion of the equatorial carbonyls toward the μ-C_2 unit of 5.2° has been calculated (see Table 2) in perfect agreement with the experimental structure (5.1°).[9] This distortion is probably due to the slight mixing of the carbonyl orbitals with the π system of C_2 (see Table 4) and could be responsible for the anomalous eclipsed conformation observed for these complexes.

Binding energy and energy decomposition analysis

The calculated binding energies (defined below) are reported in Table 6. Note that for the two series of pseudo-octahedral complexes the stability has a maximum value, respectively, for Mn

Table 6 Decomposition of the total bonding energy (eV) into contributions from different symmetries for the decomposition of all considered complexes (D_{4h} symmetry) into C_2 and the corresponding metal fragments

	$[\{M(CO)_m\}_2(\mu\text{-}C_2)]$					$[\{MCl(CO)_4\}_2(\mu\text{-}C_2)]$		
	Cr ($m = 5$)	Mn ($m = 5$)	Fe ($m = 5$)	Fe ($m = 4$)	Co ($m = 4$)	Mn	Fe	Co
$\Delta E_{a_{1g}}$	−13.3	−10.0	−4.3	−7.7	−9.0	−14.5	−10.3	−3.0
ΔE_{e_g}	−1.4	−0.7	−0.7	−0.7	−0.5	−1.6	−0.8	−0.7
$\Delta E_{a_{2u}}$	−14.9	−10.4	−10.4	−8.7	−9.6	−15.9	−10.6	−12.6
ΔE_{e_u}	+12.3	−0.5	−0.5	−0.2	−0.2	+12.5	−0.5	−0.4
$\Delta E^0 + \Delta E_{oi}$	−9.8	−10.5	−4.9	−9.6	−10.2	−10.3	−10.6	−6.3

and Fe with a d^7 metal fragment configuration and decreases both for higher and lower electron counts. This stability is even more evident if we take into account that complexes with a d^6 electron count, which have an only slightly lower binding energy, have a triplet ground state and are therefore kinetically not stable. The particular stability of the complexes with a d^7 electron count is confirmed by the high HOMO–LUMO gap calculated for compounds **1** and **2** (*ca.* 3 and 2 eV, respectively) which are by far the highest in the two series. This confirms the experimental trend by which all the synthesized complexes with a pseudo-octahedral geometry have a d^7 metal fragment configuration.

In the discussion of the bonding in these complexes it is useful to point out the relative magnitudes of the main interactions and the strengths of the bond between the two metal fragments and the central C_2 unit.[29] The total energy for dissociation of the $[\{MCl_n(CO)_{m-n}\}_2(\mu\text{-}C_2)]$ complex into a C_2 and two $MCl_n(CO)_{m-n}$ fragments can be broken down as in equation (1)[30]

$$\Delta E = \Delta E^0 + \Delta E^{prep} + \Delta E_{oi} \quad (1)$$

where ΔE^0 is the steric repulsion between the C_2 molecule and the two metal fragments, ΔE_{oi} is the orbital interaction energy and ΔE^{prep} accounts for the energy required to distort C_2 and the two fragments from their ground-state geometries to the geometries they adopt in the final complexes, in the appropriate valence states.

A better insight into the electronic factors governing the relative stability of these dinuclear complexes is provided by the analysis of the orbital interaction energy in terms of the different symmetries, equation (2). This is particularly useful for the

$$\Delta E_{oi} = \sum_{\Gamma} \Delta E_{\Gamma} \quad (2)$$

considered complexes, all of D_{4h} symmetry, as $\Delta E_{a_{1g}}$ and $\Delta E_{a_{2u}}$ represent the contributions to ΔE_{oi} due to the metal–carbon σ interactions and ΔE_{e_g} represents the contribution due to the back donation from the metal to the antibonding π* orbitals of C_2. The ΔE_{e_u} contribution represents that due to the donation from the C_2 π orbital to the empty metal orbitals; however, it gives less direct information since it is determined by a compromise between the stabilizing bonding metal–carbon π interactions in the 1π orbital and the destabilizing antibonding metal–carbon π interactions in the 3π orbital. The contributions from other symmetries are negligible.

The results of this analysis for the considered complexes of both series are reported in Table 6. We see that for complexes with d^7 and d^8 fragment configuration the stability comes essentially from the contributions of the a_{1g} and a_{2u} symmetries, associated with the metal–carbon σ bonding, which vary only slightly among the various complexes. Only in the $[\{Cr(CO)_5\}_2(\mu\text{-}C_2)]$ and $[\{MnCl(CO)_4\}_2(\mu\text{-}C_2)]$ complexes with a fragment d^6 configuration the contribution from the e_g symmetry, associated with the back donation from the metal d_π orbitals to the π* orbitals of the C_2 moiety, gives a significant stabilizing contribution, due to the higher energy of the d_π orbitals in the corresponding metal fragments. At the same time, the contribution from the e_u symmetry gives a significant destabilizing effect for these d^6 complexes. This is due to the higher energy of the metal d_π orbitals which leads to a 3π orbital with a higher metal content and then a stronger metal–carbon π-antibonding character.

Table 7 Values of $P(\sigma)$, $P(\pi)$ and $P(\pi^*)$ for complexes of the $[\{M(CO)_5\}_2(\mu\text{-}C_2)]$ (M = Cr, Mn or Fe) series

Parameter	Cr	Mn	Fe
$P(\sigma)$	0.70	0.22	0.18
$P(\pi)$	0.38	0.07	0.06
$P(\pi^*)$	0.13	0.06	0.06
$Q(C_2)$	−0.24	−0.19	−0.15

Population analysis

An alternative way of looking at the bonding in these complexes involves population analysis. Consider first the $[\{M(CO)_m\}_2(\mu\text{-}C_2)]$ (M = Cr, Mn or Fe) series; Table 7 displays the gross Mulliken populations that the most relevant C_2 fragment orbitals acquire in the complexes: $P(\sigma)$ represents the population acquired in the singly occupied C_2 orbitals of σ symmetry, a_{1g} and a_{2u}, $P(\pi)$ the population lost by the donating $1\pi_u$ orbitals, $P(\pi^*)$ the population back donated to $1\pi_g$ orbitals and $Q(C_2)$ is the charge on the C_2 unit. According to Table 7, the $C_2 \rightarrow M$ π donation and the $M \rightarrow C_2$ π*-back donation are both negligible from Mn to Co, but show a sudden increase (especially the former) in the chromium complex. Both these effects reflect the increase in the metal d_π energies which leads to higher metal character of the $9e_u$ orbital and a higher $\pi^*(C_2)$ character of the $8e_g$. At the same time the $C_2 \rightarrow M$ σ-donor contribution remains almost constant in Mn and Fe and shows a decrease in the chromium complex, essentially due to the sudden increase of the energy of the $10a_1$ level in the corresponding $Cr(CO)_5$ fragment. In all the complexes the C_2 moiety acquires a relevant negative charge (*ca.* 0.2 unit). Recalling that the HOMO has mainly a $\pi(C_2)$ character, we expect that the C_2 unit is reactive toward electrophilic attack.

A completely analogous behaviour is found when we consider the $[\{MCl(CO)_4\}_2(\mu\text{-}C_2)]$ (M = Mn, Fe or Co) series. No relevant difference is found in spite of the different oxidation states of the metals.

Conclusion

In the present investigation we have studied the factors governing the interaction mode of a bridging $\mu\text{-}C_2$ unit in dinuclear complexes of mid-to-late transition metals in low oxidation states with π-acceptor ligands. The behaviour of these complexes is very different from that of early transition metals of the titanium, vanadium and chromium triads, in high oxidation states with mainly π-donor ligands. Indeed, for the former class, only the acetylenic μ-C≡C structure has been found, irrespective of the metal d configuration, while in the latter class the d^n configuration of the metal fragment determines the interaction mode, namely M−C≡C−M, M=C=C=M or M≡C−C≡M.

Density functional calculations have been performed on two series of late transition-metal complexes and the results interpreted in terms of the simple molecular orbital model previously developed and used to predict the limiting bonding mode of the C_2 unit in the dinuclear complexes of early transition metals.[17] The parameters which have been used to predict the interaction mode of the C_2 unit are the oxidation state and the d^n configuration of the metal in the neutral metallic fragment, regardless of the values conventionally determined for the same metal parameters in the overall complex.

As long as π-acceptor ligands and late transition metals in low oxidation states are considered, only acetylenic valence-bond structures have been calculated and experimentally observed. Indeed, the metal d orbitals are filled and low in energy so that (*i*) no π donation is possible from C_2 to the filled metal d_π orbitals; (*ii*) the π-back donation from the metal to the antibonding π* orbitals of C_2 is prevented by the low energy of the d_π orbitals. Complexes corresponding to a d^7 configuration of the metal fragment have the highest HOMO–LUMO gaps and are therefore the most stable, in agreement with the special occurrence of such a configuration among the experimentally synthesized complexes. This situation is very different from that found for the early transition metals with π-donor ligands. Indeed, in that case the metal d orbitals are higher in energy and both π $C_2 \rightarrow M$ donation and $M \rightarrow C_2$ back donation can be relevant and lead for d^2 and d^3 configurations of the metal fragments to formal M=C=C=M and M≡C–C≡M valence-bond structures. These two latter bonding interactions of the C_2 unit require high and almost empty d_π orbitals which are available only in low d^n electron configurations of early transition metals and not in late transition metals in low oxidation states.

Acknowledgements

The present work has been carried out within the COST D3 Action. Support by the Fond Nationale Suisse de la Recherche Scientifique and the Consiglio Nazionale delle Ricerche is gratefully acknowledged. N. R. thanks the Herbette Foundation (Lausanne, Switzerland) for providing a research fellowship.

References

1 F. Diederich and Y. Rubin, *Angew. Chem., Int. Ed. Engl.*, 1992, **31**, 1101.
2 W. Beck, B. Niemer and M. Wieser, *Angew. Chem., Int. Ed. Engl.*, 1993, **32**, 923 and refs. therein.
3 H. Lang, *Angew. Chem., Int. Ed. Engl.*, 1994, **34**, 547.
4 D. R. Neithamer, R. E. LaPointe, R. A. Wheeler, D. S. Richeson, G. D. Van Duyne and P. T. Wolczanski, *J. Am. Chem. Soc.*, 1989, **111**, 9056.
5 K. G. Caulton, R. H. Cayton, R. H. Chisholm, J. C. Huffman, E. B. Lobkovsky and Z. Xue, *Organometallics*, 1992, **11**, 321.
6 S. De Angelis, E. Solari, C. Floriani, A. Chiesi-Villa and R. Rizzoli, *Angew. Chem., Int. Ed. Engl.*, 1995, **34**, 1092.
7 P. Binger, P. Müller, P. Philipps, G. Gabor, R. Mynott, A. T. Herrmann, F. Langhauser and C. Krüger, *Chem. Ber.*, 1992, **125**, 2209.
8 J. Heidrich, M. Stelman, M. Appel, W. Beck, J. R. Phillips and W. C. Trogler, *Organometallics*, 1990, **9**, 1296.
9 J. A. Davies, M. El-Ghanam, A. A. Pinkerton and D. A. Smith, *J. Organomet. Chem.*, 1991, **409**, 367.
10 G. A. Koutsantonis and J. P. Selegue, *J. Am. Chem. Soc.*, 1991, **113**, 2316.
11 F. R. Lemke, D. J. Szalda and R. M. Bullock, *J. Am. Chem. Soc.*, 1991, **113**, 8466.
12 M.-C. Cen, Y.-J. Tsai, C.-T. Chen, Y.-C. Lin, T.-W. Tseng, G.-H. Lee and Y. Wang, *Organometallics*, 1991, **10**, 378.
13 N. A. Ustynyuk, U. N. Vinogradova and D. N. Kravtsov, *Organomet. Chem. USSR*, 1988, **1**, 45.
14 H. Ogawa, K. Onitsuka, T. Joh, S. Takahashi, Y. Yamamoto and H. Yamazaki, *Organometallics*, 1988, **7**, 2257.
15 R. J. Cross and M. F. Davidson, *J. Chem. Soc., Dalton Trans.*, 1986, 411.
16 M. Akita, M. Terada, S. Oyama, S. Sugimoto and Y. Moro-oka, *Organometallics*, 1991, **10**, 1561.
17 P. Belanzoni, N. Re, M. Rosi, A. Sgamellotti and C. Floriani, *Organometallics*, 1996, **15**, 4264.
18 J. Chatt, R. C. Fay and R. L. Richards, *J. Chem. Soc. A*, 1971, 2399; J. M. Treitel, M. T. Flood, R. E. March and H. B. Gray, *J. Am. Chem. Soc.*, 1969, **91**, 6512; D. Sellmann, *Angew. Chem., Int. Ed. Engl.*, 1974, **13**, 639.
19 N. Re, M. Rosi, A. Sgamellotti, C. Floriani and E. Solari, *Inorg. Chem.*, 1994, **33**, 4390.
20 N. Re, M. Rosi, A. Sgamellotti and C. Floriani, *Inorg. Chem.*, 1995, **34**, 3410.
21 C. B. Powell and M. B. Hall, *Inorg. Chem.*, 1984, **23**, 4619.
22 E. J. Baerends, D. E. Ellis and P. Ros, *Chem. Phys.*, 1973, **2**, 42; E. J. Baerends and P. Ros, *Chem. Phys.*, 1973, **2**, 51; 1975, **8**, 41; *Int. J. Quantum Chem.*, 1978, **S12**, 169.
23 P. M. Boerrigter, G. te Velde and E. J. Baerends, *Int. J. Quantum Chem.*, 1988, **33**, 87; G. Te Velde and E. J. Baerends, *J. Comput. Phys.*, 1992, **99**, 84.
24 T. Ziegler, V. Tschinke, E. J. Baerends, J. G. Snijders and W. Ravenek, *J. Phys. Chem.*, 1989, **93**, 3050.
25 S. H. Vosko, L. Wilk and M. Nusair, *Can. J. Phys.*, 1980, **58**, 1200.
26 A. D. Becke, *Phys. Rev. A*, 1988, **38**, 2398.
27 J. P. Perdew, *Phys. Rev. B*, 1986, **33**, 8822.
28 L. Versluis and T. Ziegler, *J. Chem. Phys.*, 1988, **88**, 322.
29 T. A. Albright, J. K. Burdett and M. H. Whangbo, *Orbital Interactions in Chemistry*, Wiley, New York, 1985.
30 T. Ziegler, *A General Energy Decomposition Scheme for the Study of Metal–Ligand Interactions in Complexes, Clusters and Solids*, NATO ASI C378, Kluwer, Boston, MA, 1992.

Received 25*th June* 1997; *Paper* 7/04480A